

# MRI Brain Image Segmentation by Fuzzy Symmetry Based Genetic Clustering Technique

Sriparna Saha, *Student Member, IEEE* and Sanghamitra Bandyopadhyay, *Senior Member, IEEE*  
Machine Intelligence Unit, Indian Statistical Institute, Kolkata, India-700108  
Email: {sriparna\_r, sanghami}@isical.ac.in

**Abstract**—In this paper, an automatic segmentation technique of multispectral magnetic resonance image of the brain using a new fuzzy point symmetry based genetic clustering technique is proposed. The proposed real-coded variable string length genetic fuzzy clustering technique (Fuzzy-VGAPS) is able to evolve the number of clusters present in the data set automatically. Here assignment of points to different clusters are made based on the point symmetry based distance rather than the Euclidean distance. The cluster centers are encoded in the chromosomes, whose value may vary. A newly developed fuzzy point symmetry based cluster validity index, *FSym*-index, is used as a measure of ‘goodness’ of the corresponding partition. This validity index is able to correctly indicate presence of clusters of different sizes as long as they are internally symmetrical. A Kd-tree based data structure is used to reduce the complexity of computing the symmetry distance. The proposed method is applied on several simulated T1-weighted, T2-weighted and proton density normal and MS lesion magnetic resonance brain images. Superiority of the proposed method over Fuzzy C-means, Expectation Maximization, Fuzzy Variable String Length Genetic Algorithm (Fuzzy-VGA) clustering algorithms are demonstrated quantitatively. The automatic segmentation obtained by Fuzzy-VGAPS clustering technique is also compared with the available ground truth information.

**Keywords:** Unsupervised classification, fuzzy clustering, cluster validity index, symmetry, point symmetry based distance, Kd tree, magnetic resonance image

## I. INTRODUCTION

Segmentation is a process of partitioning an image space into some non-overlapping meaningful homogeneous regions [1]. In general, these regions will have a strong correlation with the objects in the image. The success of an image analysis system depends on the quality of segmentation. In the analysis of medical images for computer-aided diagnosis and therapy, segmentation is often required as a preliminary processing task. Medical image segmentation is a complex and challenging task due to the intrinsically imprecise nature of the images.

Fully automatic brain tissue classification from magnetic resonance images (MRI) is of great importance for research and clinical study of much neurological pathology. The accurate segmentation of MR images into different tissue classes, especially gray matter (GM), white matter (WM) and cerebrospinal fluid (CSF), is an important task. Moreover, regional volume calculations may bring even more useful diagnostic information. Among them, the quantization of gray and white matter volumes may be of major interest in neurodegenerative disorders such as Alzheimer disease,

in movement disorders such as Parkinson or Parkinson related syndrome, in white matter metabolic or inflammatory disease, in congenital brain malformations or perinatal brain damage, or in post traumatic syndrome.

The automatic segmentation of brain MR images, however, remains a persistent problem. Automated and reliable tissue classification is further complicated by overlap of MR intensities of different tissue classes and by the presence of a spatially smoothly varying intensity inhomogeneity. Statistical approaches are often used for MR image segmentation. This type of method labels pixels according to probability values, which are determined based on the intensity distribution of the image. Hidden Markov Random Field (HMRF) model has also been used for MRI image segmentation where it is combined with the Expectation Maximization (EM) algorithm [2] to estimate the involved model parameters [3][4]. Clustering approaches have been widely used for segmentation of MRI brain image. Unsupervised clustering method has high reproducibility because its results are mainly based on the information of image data itself, and it requires little or no assumption of the model, and the distribution of the image data. The use of neural networks, evolutionary computation and/or fuzzy clustering techniques for MRI image segmentation has been investigated in [5] [6].

In order to cluster a data set, some similarity or dissimilarity criteria has to be defined. The measure of similarity is data dependent. It may be noted that one of the basic feature of shapes and objects is symmetry. A new type of non-metric distance, based on point symmetry, is proposed in [7] and thereafter it is modified in [8]. It has been shown in [9] that the PS distance proposed in [8] also has some serious drawbacks and a new PS distance ( $d_{ps}$ ) is defined in [9] in order to remove these drawbacks. For reducing complexity of point symmetry distance computation, *Kd-tree* based data structure is used.

The main contribution of this present paper is a novel method for fully automatic brain image segmentation. In this article a fuzzy variable string length genetic point symmetry (Fuzzy-VGAPS) based clustering technique is proposed which is then used to automatically segment the brain image. Here membership values of points to different clusters are computed based on a newly proposed point symmetry based distance rather than the Euclidean distance. This enables the proposed algorithm to automatically evolve the appropriate clustering of all types of clusters, both convex and non convex, which have some symmetrical structures.

The chromosome encodes the centres of a number of clusters, whose value may vary. A new fuzzy cluster validity index named *FSym*-index is proposed here and thereafter it is utilized for computing the fitness of the chromosomes. *FSym*-index uses the newly developed point symmetry based distance to measure the ‘goodness’ of a particular cluster in terms of cluster symmetry. The effectiveness of the proposed algorithm is shown in segmenting the MRI images of the normal brain and MRI brain images with multiple sclerosis lesions. The segmentation results are then compared with the available ground truth information. For the purpose of comparison, the well-known Fuzzy C-means algorithm [10] and the Expectation Maximization (EM) [11] clustering algorithm are also executed, firstly with the number of clusters automatically determined by the Fuzzy-VGAPS and then with the actual number of clusters present in the images. The segmentation results are compared with that provided by Fuzzy-VGAPS clustering algorithm quantitatively. In a part of the experiment, fuzzy variable string length genetic algorithm (Fuzzy-VGA) [12] which uses the Euclidean distance for computing the membership values of points to different clusters is also executed on the MRI brain images to automatically segment it. The results are also compared with those obtained by Fuzzy-VGAPS clustering technique.

## II. FUZZY-VGAPS CLUSTERING: FUZZY VARIABLE STRING LENGTH GENETIC POINT SYMMETRY BASED CLUSTERING TECHNIQUE

In this section, the use of variable string length genetic algorithm using a newly developed point symmetry based distance is proposed for automatically determining the optimum fuzzy partition of an image-data. Here we have considered the best partition to be the one that corresponds to the maximum value of the proposed *FSym*-index which is defined later. Here both the number of clusters as well as the appropriate fuzzy clustering of the data are evolved simultaneously using the search capability of genetic algorithms. In this section the term ‘data’ means the image data, where each point corresponds to each pixel present in the image. The feature vector of each pixel is composed of the intensity values at different bands of the image.

For the purpose of clustering, each chromosome in the population of GA encodes a possible partitioning of the data, the goodness of which is computed as a function of an appropriate cluster validity index. This index must be optimized in order to obtain the best partitions. Since the number of clusters is considered to be variable, the string lengths of different chromosomes in the same population are allowed to vary. As a consequence, the crossover and mutation operators are suitably modified in order to tackle the concept of variable length chromosomes. The technique is described below in detail.

### A. String Representation and Population Initialization

In Fuzzy-VGAPS clustering, the chromosomes are made up of real numbers which represent the coordinates of the centers of the partitions. If chromosome  $i$  encodes the centers

of  $K_i$  clusters in  $d$  dimensional space then its length  $l_i$  is taken to be  $d * K_i$ . Each center is considered to be indivisible. Each string  $i$  in the population initially encodes the centers of a number,  $K_i$ , of clusters, such that  $K_i = (\text{rand}() \bmod K^*) + 2$ . Here,  $\text{rand}()$  is a function returning an integer, and  $K^*$  is a soft estimate of the upper bound of the number of clusters. The number of clusters will therefore range from 2 to  $K^* + 1$ . The  $K_i$  centers encoded in a chromosome are randomly selected distinct points from the data set. These selected points are then distributed randomly in the chromosome. Thereafter five iterations of the  $K$ -means algorithm is executed with the set of centers encoded in each chromosome. The resultant centers are used to replace the centers in the corresponding chromosomes. This makes the centers separated initially.

### B. Fitness Computation

This is composed of two steps. Firstly membership values of  $n$  points to different clusters are computed by using the newly developed point symmetry based distance  $d_{ps}$ . Next, the *FSym*-index is computed and used as a measure of the fitness of the chromosome.

1) *A New Definition of the Point Symmetry Distance:* The newly developed point symmetry (PS) distance [9],  $d_{ps}(\bar{x}, \bar{c})$ , is associated with point  $\bar{x}$  with respect to a center  $\bar{c}$ . The proposed point symmetry distance is defined as follows: Let a point be  $\bar{x}$ . The symmetrical (reflected) point of  $\bar{x}$  with respect to a particular centre  $\bar{c}$  is  $2 \times \bar{c} - \bar{x}$ . Let us denote this by  $\bar{x}^*$ . Let  $knear$  unique nearest neighbors of  $\bar{x}^*$  be at Euclidean distances of  $d_i, i = 1, 2, \dots, knear$ . Then

$$d_{ps}(\bar{x}, \bar{c}) = d_{sym}(\bar{x}, \bar{c}) \times d_e(\bar{x}, \bar{c}), \quad (1)$$

$$= \frac{\sum_{i=1}^{knear} d_i}{knear} \times d_e(\bar{x}, \bar{c}), \quad (2)$$

where  $d_e(\bar{x}, \bar{c})$  is the Euclidean distance between the point  $\bar{x}$  and  $\bar{c}$ . It can be seen from Equation 2 that  $knear$  cannot be chosen equal to 1, since if  $\bar{x}^*$  exists in the data set then  $d_{ps}(\bar{x}, \bar{c}) = 0$  and hence there will be no impact of the Euclidean distance. On the contrary, large values of  $knear$  may not be suitable because it may overestimate the amount of symmetry of a point with respect to a particular cluster center. Here  $knear$  is chosen equal to 2.

Note that  $d_{ps}(\bar{x}, \bar{c})$ , which is a non-metric, is a way of measuring the amount of symmetry between a point and a cluster center, rather than the distance like any Minkowski distance.

The basic differences between the PS-distances in [7] and [8], and the proposed  $d_{ps}(\bar{x}, \bar{c})$  are as follows:

- 1) Instead of computing the Euclidean distance between the original reflected point  $\bar{x}^* = 2 \times \bar{c} - \bar{x}$  and its first nearest neighbor as in [7] and [8], here the average distance between  $\bar{x}^*$  and its  $knear$  unique nearest neighbors have been taken. Consequently this term will never be equal to 0, and the effect of  $d_e(\bar{x}, \bar{c})$ , the Euclidean distance, will always be considered. Note

that if only the nearest neighbor of  $\bar{x}^*$  is considered and this happens to coincide with  $\bar{x}^*$ , then this term will be 0, making the distance insensitive to  $d_e(\bar{x}, \bar{c})$ . But considering  $knear$  nearest neighbors will reduce these problems.

- 2) Considering the  $knear$  nearest neighbors in the computation of  $d_{ps}$  makes the PS-distance more robust and noise resistant. From an intuitive point of view, if this term is less, then the likelihood that  $\bar{x}$  is symmetrical with respect to  $\bar{c}$  increases. This is not the case when only the first nearest neighbor is considered which could mislead the method in noisy situations.

Note that the complexity of computing  $d_{ps}(\bar{x}, \bar{c})$  is  $O(n)$ , where  $n$  is the total number of data points. For all the  $n$  points and  $K$  clusters, the complexity becomes  $O(n^2K)$ . In order to reduce this, we have used Kd-tree based nearest neighbor search, ANN (Approximate Nearest Neighbor), which is a library written in C++ (obtained from <http://www.cs.umd.edu/~mount/ANN>). Here ANN is used to find exact  $d_i$ s,  $i = 1$  to  $knear$  in Equation 2 efficiently. The Kd-tree structure can be constructed in  $O(n \log n)$  time and takes  $O(n)$  space.

2) *Computing the Membership Values:* For each point  $\bar{x}_j, j = 1, 2, \dots, n$ , the membership values to  $K$  different clusters are calculated in the following way. Find the cluster center nearest to  $\bar{x}_j$  in the symmetrical sense. That is, we find the cluster center  $k$  that is nearest to the input pattern  $\bar{x}_j$  using the minimum-value criterion:  $k = \text{Argmin}_{i=1, \dots, K} d_{ps}(\bar{x}_j, \bar{c}_i)$  where the point symmetry based distance  $d_{ps}(\bar{x}_j, \bar{c}_i)$  is computed by Equation 2. Here,  $\bar{c}_i$  denotes the center of the  $i$ th cluster. If the corresponding  $d_{sym}(\bar{x}_j, \bar{c}_k)$  (as defined in Equation 1) is smaller than a pre-specified parameter  $\theta$ , then we update the membership  $u_{ij}$  using the following criterion:  $u_{ij} = 1$ , if  $i = k$  and  $u_{ij} = 0$ , if  $i \neq k$ . Otherwise, we update the membership  $u_{ij}$  by using the following rule which corresponds to the normal Fuzzy C-Means [10] algorithm:

$$u_{ij} = \frac{1}{\sum_{i=1}^K \left( \frac{d_{ij}}{d_{kj}} \right)^{\frac{2}{m-1}}}$$

where  $m \in [2, \infty)$  is a weighting exponent called the fuzzifier. Here we have chosen  $m = 2$ .  $d_{ij}$  represents the distance from a pattern  $\bar{x}_j$  to the cluster center  $\bar{c}_i$ . The value of  $\theta$  is kept equal to the maximum nearest neighbor distance among all the points in the data set. It may be noted that if a point is indeed symmetric with respect to some cluster center then the symmetrical distance computed in the above way will be small, and can be bounded as follows. Let  $d_{NN}^{max}$  be the maximum nearest neighbor distance in the data set. That is  $d_{NN}^{max} = \max_{i=1, \dots, N} d_{NN}(\bar{x}_i)$ , where  $d_{NN}(\bar{x}_i)$  is the nearest neighbor distance of  $\bar{x}_i$ . Assuming that reflected point of  $\bar{x}$  with respect to the cluster centre  $\bar{c}$  lies within the data space, it may be noted that  $d_1 \leq \frac{d_{NN}^{max}}{2}$  and  $d_2 \leq \frac{3d_{NN}^{max}}{2}$ , resulting in  $\frac{d_1+d_2}{2} \leq d_{NN}^{max}$ . Here  $d_i$ s,  $i = 1, \dots, knear$  are Euclidean distances of the  $knear$  nearest neighbors of  $\bar{x}_i^*$  (the reflected point of  $\bar{x}_i$  with respect to cluster center  $\bar{c}$ ). Ideally,

a point  $\bar{x}$  is exactly symmetrical with respect to some  $\bar{c}$  if  $d_1 = 0$ . However considering the uncertainty of the location of a point as the sphere of radius  $d_{NN}^{max}$  around  $\bar{x}$ , we have kept the threshold  $\theta$  equals to  $d_{NN}^{max}$ . Thus the computation of  $\theta$  is automatic and does not require user intervention.

3) *Updating the Centers:* The centers encoded in a chromosome are updated using the following equation as in Fuzzy C-means [10]

$$\bar{c}_i = \frac{\sum_{j=1}^n (u_{ij})^m \bar{x}_j}{\sum_{j=1}^n (u_{ij})^m}, \quad 1 \leq i \leq K.$$

4) *Fitness Calculation:* The fitness of a chromosome is computed using the  $FSym$ -index. Let  $K$  cluster centres be denoted by  $\bar{c}_i$  where  $1 \leq i \leq K$  and  $U(X) = [u_{ij}]_{K \times n}$  is a partition matrix for the data. Then  $FSym$ -index is defined as follows:

$$FSym(K) = \left( \frac{1}{K} \times \frac{1}{\mathcal{E}_K} \times D_K \right), \quad (3)$$

where  $K$  is the number of clusters. Here,  $\mathcal{E}_K = \sum_{i=1}^K E_i$  such that  $E_i = \sum_{j=1}^n (u_{ij} \times d_{ps}(\bar{x}_j, \bar{c}_i))$  and  $D_K = \max_{i,j=1}^K \|\bar{c}_i - \bar{c}_j\|$ .  $D_K$  is the maximum Euclidean distance between two cluster centers among all centers.  $d_{ps}(\bar{x}_j, \bar{c}_i)$  is computed by Equation 2.

The objective is to maximize the  $FSym$ -index in order to obtain the actual number of clusters and to achieve proper clustering. As formulated in Equation 3,  $FSym$  is a composition of three factors, these are  $1/K$ ,  $1/\mathcal{E}_K$  and  $D_K$ . The first factor increases as  $K$  decreases; as  $FSym$  needs to be maximized for optimal clustering, so it will prefer to decrease the value of  $K$ . The second factor is the within cluster total symmetrical distance. For clusters which have good symmetrical structure,  $E_i$  value is less. This, in turn, indicates that formation of more number of clusters, which are symmetrical in shape, would be encouraged. Finally the third factor,  $D_K$ , measuring the maximum separation between a pair of clusters, increases with the value of  $K$ . As these three factors are complementary in nature, so they are expected to compete and balance each other critically for determining the proper partitioning.

The use of  $D_K$ , as the measure of separation, requires further elaboration. Instead of using the maximum separation between two clusters, several other alternatives could have been used. For example, if  $D_K$  was the sum of pairwise inter cluster distances in a  $K$ -cluster structure, then it would increase largely with increase in the value of  $K$ . This might lead to the formation of maximum possible number of clusters equal to the number of elements in the data set. If  $D_K$  was the average inter cluster distance then it would decrease at each step with  $K$ , instead of being increased. So, this will only leave us with the minimum possible number of clusters. The minimum distance between two clusters may be another choice for  $D_K$ . However, this measure would also decrease significantly with increase in the number of clusters. So this would lead to a structure where the loosely connected sub-structures remain as they were, where in fact a separation was expected. Thus maximum separability may

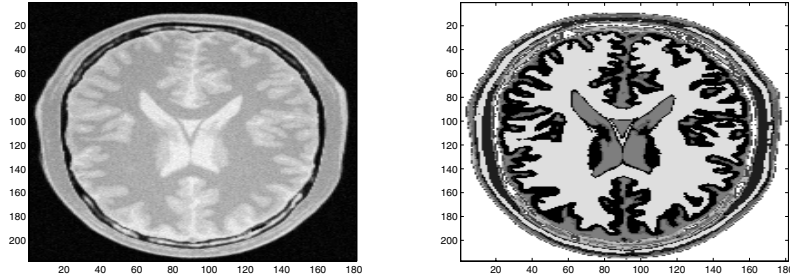


Fig. 1. (a) Original T1-weighted MRI image of the normal brain in z1 plane (b) Segmentation obtained by Fuzzy-VGAPS clustering

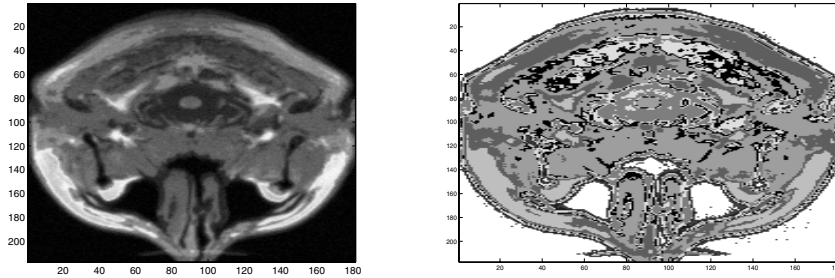


Fig. 2. (a) Original T1-weighted MRI image of the normal brain in z2 plane (b) Segmentation obtained by Fuzzy-VGAPS clustering

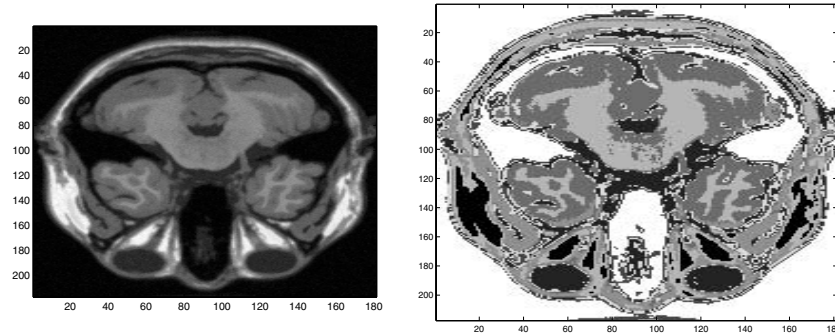


Fig. 3. (a) Original T1-weighted MRI image of the normal brain in z36 plane (b) Segmentation obtained by Fuzzy-VGAPS clustering

not be attained. In contrast, if we consider the maximum inter cluster separation then we see that this tends to increase significantly until we reach the maximum separation among compact clusters and then it becomes almost constant. The upper bound of this value, which is equal to the maximum separation between two points, is only attainable when we have two extreme data elements as two single element clusters. But the terminating condition is reached well before this situation. This is the reason why we try to improve the maximum distance between two maximally separated clusters.

The fitness function for chromosome  $j$  is defined as  $FSym_j$  i.e., the  $FSym$  index computed for the chromosome. The objective of GA is to maximize this fitness function.

### C. Selection

Conventional proportional selection is applied on the population of strings. Here, a string receives a number of copies that is proportional to its fitness in the population. We have used roulette wheel strategy for implementing the proportional selection scheme.

### D. Crossover

For the purpose of crossover, the cluster centers are considered to be indivisible, i.e., the crossover points can only lie in between two cluster centers. The crossover operation, applied stochastically, must ensure that information exchange takes place in such a way that both the offspring encode the centers of at least two clusters. For this, the operator is defined as follows [12]: Let parent chromosomes  $P_1$  and  $P_2$  encode  $M_1$  and  $M_2$  cluster centers respectively.  $\tau_1$ , the crossover point in  $P_1$ , is generated as  $\tau_1 = \text{rand}() \bmod M_1$ .

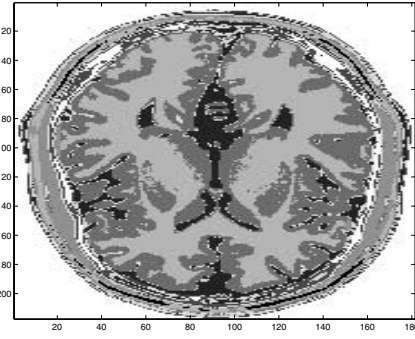
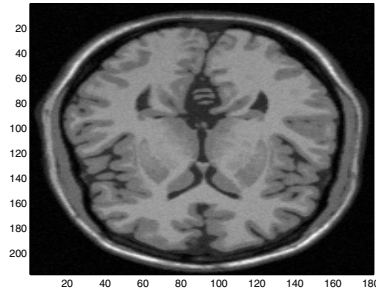


Fig. 4. (a) Original T1-weighted MRI image of the normal brain in z72 plane (b) Segmentation obtained by Fuzzy-VGAPS clustering

Let  $\tau_2$  be the crossover point in  $P_2$ , and it may vary in between  $[\text{LB}(\tau_2), \text{UB}(\tau_2)]$ , where  $\text{LB}(\tau_2)$  and  $\text{UB}(\tau_2)$  indicate the lower and upper bounds of the range of  $\tau_2$  respectively.  $\text{LB}(\tau_2)$  and  $\text{UB}(\tau_2)$  are given by  $\text{LB}(\tau_2) = \min[2, \max[0, 2 - (M_1 - \tau_1)]]$  and  $\text{UB}(\tau_2) = [M_2 - \max[0, 2 - \tau_1]]$ . Therefore  $\tau_2$  is given by

$$\begin{aligned} \tau_2 &= \text{LB}(\tau_2) + \text{rand}() \text{mod}(\text{UB}(\tau_2) - \text{LB}(\tau_2)) \\ &\quad \text{if}(\text{UB}(\tau_2) \geq \text{LB}(\tau_2)), \\ &= 0 \quad \text{otherwise.} \end{aligned}$$

It can be verified by some simple calculations that if the crossover points  $\tau_1$  and  $\tau_2$  are chosen according to the above rules, then none of the offspring generated would have less than two clusters.

Crossover probability is selected adaptively as in [13]. The expressions for crossover probabilities are computed as follows. Let  $f_{max}$  be the maximum fitness value of the current population,  $\bar{f}$  be the average fitness value of the population and  $f'$  be the larger of the fitness values of the solutions to be crossed. Then the probability of crossover,  $\mu_c$ , is calculated as:

$$\begin{aligned} \mu_c &= k_1 \times \frac{(f_{max} - f')}{(f_{max} - \bar{f})}, \text{ if } f' > \bar{f}, \\ \mu_c &= k_3, \text{ if } f' \leq \bar{f}. \end{aligned}$$

Here, as in [13], the values of  $k_1$  and  $k_3$  are kept equal to 1.0. Note that, when  $f_{max} = \bar{f}$ , then  $f' = f_{max}$  and  $\mu_c$  will be equal to  $k_3$ . The value of  $\mu_c$  is increased when the better of the two chromosomes to be crossed is itself quite poor. In contrast when it is a good solution,  $\mu_c$  is low so as to reduce the likelihood of disrupting a good solution by crossover.

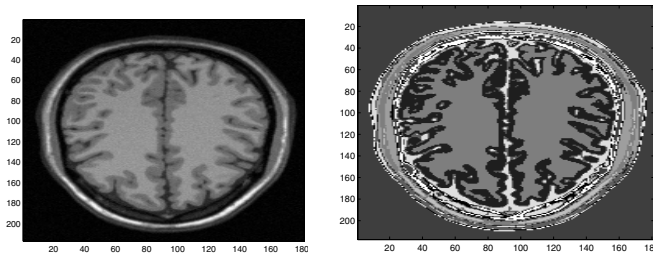


Fig. 5. (a) Original T1-weighted MRI image of the normal brain in z108 plane (b) Segmentation obtained by Fuzzy-VGAPS clustering

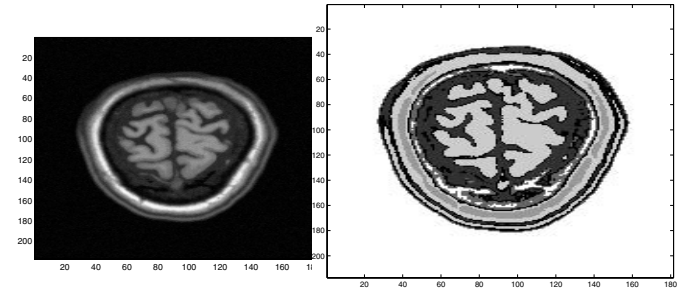


Fig. 6. (a) Original T1-weighted MRI image of the normal brain in z144 plane (b) Segmentation obtained by Fuzzy-VGAPS clustering

### E. Mutation

Mutation is applied on each chromosome with probability  $\mu_m$ . Mutation is of three types. (1) Each valid position (which contains some cluster center) in a chromosome is mutated with probability  $\mu_m$  in the following way. The valid position is replaced with a random variable drawn from a Laplacian distribution,  $p(\epsilon) \propto e^{-\frac{|\epsilon - \mu|}{\delta}}$ , where the scaling factor  $\delta$  sets the magnitude of perturbation. Here  $\mu$  is the value at the position which is to be perturbed. The scaling factor  $\delta$  is chosen equal to 1.0. The old value at the position is replaced with the newly generated value. (2) One randomly generated valid position is removed and replaced by '#' (here '#' sign corresponds to some invalid position which does not contain any cluster center, during computation the position containing '#' sign is ignored). (3) One randomly chosen invalid position is replaced by randomly chosen point from the data set.

Any one of the above mentioned types of mutation is applied randomly on a particular chromosome if it is selected for mutation.

The mutation probability is also selected adaptively for each chromosome as in [13]. The expression for mutation probability,  $\mu_m$ , is given below:

$$\begin{aligned} \mu_m &= k_2 \times \frac{(f_{max} - \bar{f})}{(f_{max} - \bar{f})} \text{ if } f > \bar{f}, \\ \mu_m &= k_4 \text{ if } f \leq \bar{f}. \end{aligned}$$

Here, values of  $k_2$  and  $k_4$  are kept equal to 0.5. This adaptive mutation helps GA to avoid getting stuck at local optimum. When GA converges to a local optimum, i.e., when  $f_{max} - \bar{f}$  decreases,  $\mu_c$  and  $\mu_m$  both will be increased. This may help

TABLE I

MINKOWSKI SCORES (MS) OBTAINED BY FCM, EM AND FUZZY-VGAPS CLUSTERING ALGORITHMS ON SIMULATED MRI VOLUMES FOR NORMAL BRAIN PROJECTED ON DIFFERENT Z PLANES. HERE # AC, # OC DENOTES, RESPECTIVELY, THE ACTUAL NUMBER OF CLUSTERS AND THE AUTOMATICALLY OBTAINED NUMBER OF CLUSTERS (AFTER APPLICATION OF FUZZY-VGAPS). FUZZY-VGAPS IS DENOTED BY 'FVGAPS'.

z plane	#AC	MS for AC		#OC	MS for OC		
		FCM	EM		FCM	EM	FVAGPS
1	6	1.08	1.05	9	0.70	1.019	0.69
2	6	0.76	0.78	9	0.65	0.83	0.62
3	6	0.57	0.76	8	0.62	0.64	0.59
36	9	0.89	0.98	8	0.88	1.12	0.84
72	10	0.75	0.74	8	0.72	0.70	0.59
108	9	0.79	0.58	9	0.79	0.58	0.52
144	9	0.82	0.72	6	0.34	0.76	0.33

TABLE II

MINKOWSKI SCORES (MS) OBTAINED BY FCM, EM AND FUZZY-VGAPS CLUSTERING ALGORITHMS ON SIMULATED MRI VOLUMES FOR BRAIN WITH MULTIPLE SCLEROSIS LESIONS PROJECTED ON DIFFERENT Z PLANES. HERE # AC, # OC DENOTES, RESPECTIVELY, THE ACTUAL NUMBER OF CLUSTERS AND THE AUTOMATICALLY OBTAINED NUMBER OF CLUSTERS (AFTER APPLICATION OF FUZZY-VGAPS). FUZZY-VGAPS IS DENOTED BY 'FVGAPS'.

z plane	AC	MS for AC		OC	MS for OC		
		FCM	EM		FCM	EM	FVAGPS
1	6	0.59	0.59	10	0.74	0.66	0.58
2	6	0.75	0.76	10	0.75	0.67	0.58
5	6	0.74	0.76	8	0.69	0.77	0.62
36	9	0.99	1.01	9	0.99	1.01	0.81
72	11	0.72	0.63	11	0.72	0.63	0.62
108	10	0.78	0.58	9	0.79	0.70	0.57
144	9	0.31	0.76	10	0.80	0.81	0.31

GA to come out of local optimum.

#### F. Termination

In this paper, we have executed the algorithm for a fixed number of generations. Moreover, the elitist model of GAs has been used, where the best string seen so far is stored in a location within the population. The best string of the last generation provides the solution to the clustering problem.

### III. EXPERIMENTAL RESULTS

The MRI image of the brain chosen for the experiment is available in three bands:  $T_1$ -weighted, proton density ( $p_d$ )-weighted and  $T_2$ -weighted. The normal brain images are obtained from Brainweb database [14]. The images correspond to the 1 mm slice thickness, 3% noise (calculated relative to the brightest tissue) and with 20% intensity non-uniformity. The image of size  $217 \times 181$  is available in 181 different z planes. The proposed clustering algorithm is executed on 7 of these z planes. The algorithm is applied to a particular z plane at a time to get the clusters and the cluster centers. The parameters of the Fuzzy-VGAPS algorithm are as follows: population size=20, total number of generations=15. The mutation and crossover probabilities are calculated adaptively. Number of clusters,  $K$ , is varied from 2 to 20. For the normal MRI brain image, the ground truth

TABLE III

THE AUTOMATICALLY OBTAINED CLUSTER (OC) NUMBER AND THE CORRESPONDING MINKOWSKI SCORES (MS) AFTER APPLICATION OF FUZZY-VGA AND FUZZY-VGAPS CLUSTERING ALGORITHMS ON SIMULATED MRI VOLUMES FOR BRAIN WITH MULTIPLE SCLEROSIS LESIONS PROJECTED ON FIRST 10 Z PLANES.

z plane no.	AC	Fuzzy-VGA		Fuzzy-VGAPS	
		OC	MS	OC	MS
1	6	2	1.21	10	0.58
2	6	2	1.20	10	0.58
3	6	2	1.19	7	0.71
4	6	5	0.69	5	0.67
5	6	2	1.184	8	0.62
6	6	2	1.18	3	0.71
7	6	2	1.17	8	0.70
8	6	2	1.16	9	0.71
9	6	2	1.16	9	0.68
10	9	2	1.17	9	0.65

information is available to us. There are a total of 10 classes present in the images. But the number of classes varies along the different z planes. Ten classes are Background, CSF, Grey Matter, White Matter, Fat, Muscle/Skin, Skin, Skull, Glial Matter and Connective. Table I shows the actual number of clusters and the number of clusters automatically determined by the proposed Fuzzy-VGAPS clustering technique (after application on the above mentioned brain images projected on different z-planes). In order to measure the segmentation solution quantitatively, we have also calculated *Minkowski Score*(MS) [15]. This is a measure of the quality of a solution given the true clustering. Let T be the "true" solution and S the solution we wish to measure. Denote by  $n_{11}$  the number of pairs of elements that are in the same cluster in both S and T. Denote by  $n_{01}$  the number of pairs that are in the same cluster only in S, and by  $n_{10}$  the number of pairs that are in the same cluster in T. *Minkowski Score* (MS) is then defined as:  $MS(T, S) = \sqrt{\frac{n_{01} + n_{10}}{n_{11} + n_{10}}}$ . For MS, the optimum score is 0, with lower scores being "better". The MS scores obtained by Fuzzy-VGAPS clustering corresponding to the 7 brain images are also reported in Table I. For the purpose of comparison, we have executed Fuzzy C-means [10] and Expectation Maximization (EM) [11] algorithms on the above mentioned brain datasets with two different  $K$  values. In the first case,  $K$  is equal to the actual cluster number that present in that particular plane. Next, it is set equal to that automatically determined by Fuzzy-VGAPS algorithm. The corresponding MS scores of all the above runs of both the comparing algorithms are also reported in Table I for all the 7 images. Results show that the MS-score corresponding to the partitioning provided by the Fuzzy-VGAPS clustering, in general, is the minimum among all the partitions. This implies the superior performance of Fuzzy-VGAPS in automatically detecting the proper partitioning from the MRI normal brain images. Figures 1(a), 2(a), 3(a), 4(a), 5(a), 6(a) show the original MRI normal brain images in T1 band in z1, z2, z36, z72, z108, z144 planes, respectively. Figures 1(b), 2(b), 3(b), 4(b), 5(b), 6(b) show, respectively, the corresponding segmented images obtained

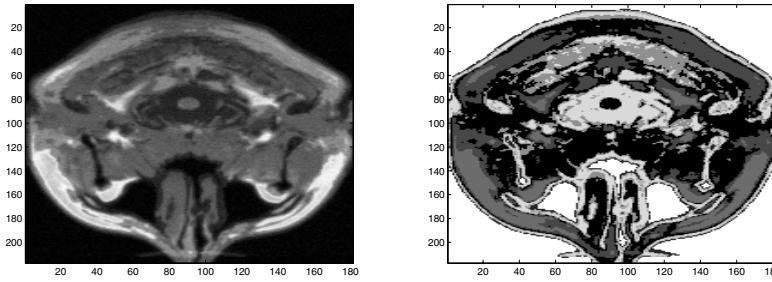


Fig. 7. (a) Original T1-weighted MRI image of the brain with Multiple Sclerosis Lesions in z2 plane (b) Segmentation obtained by Fuzzy-VGAPS

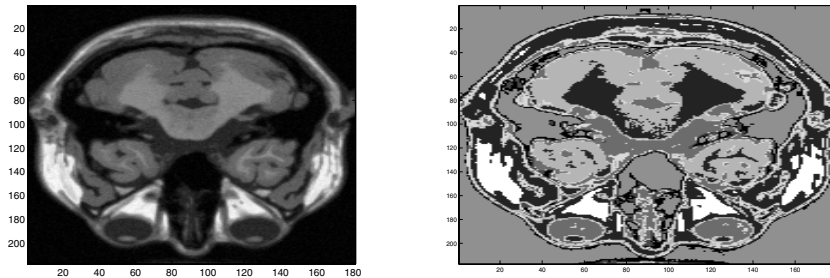


Fig. 8. (a) Original T1-weighted MRI image of the brain with Multiple Sclerosis Lesions in z36 plane (b) Segmentation obtained by Fuzzy-VGAPS

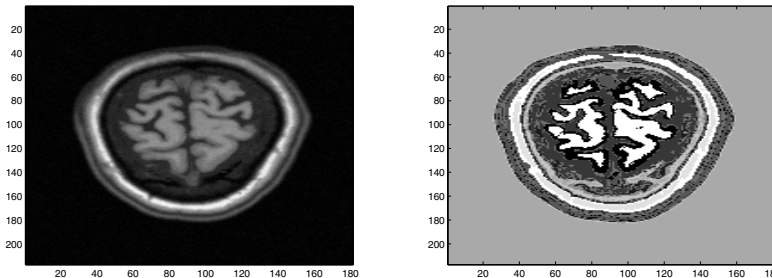


Fig. 9. (a) Original T1-weighted MRI image of the brain with Multiple Sclerosis Lesions in z144 plane (b) Segmentation obtained by Fuzzy-VGAPS

after application of Fuzzy-VGAPS clustering algorithm. Due to lack of space, the corresponding segmented images obtained by FCM and EM algorithms are not provided. Next, the proposed algorithm is executed on some simulated MRI volumes for brain with multiple sclerosis lesions obtained from [14]. These images are again available in 3 modalities  $T_1$ -weighted, proton density ( $p_d$ )-weighted and  $T_2$ -weighted. These images also correspond to 1 mm slice thickness, 3% noise (calculated relative to the brightest tissue) and with 20% intensity non-uniformity. Now, the images contain a total of 11 classes. These are Background, CSF, Grey Matter, White Matter, Fat, Muscle/Skin, Skin, Skull, Glial Matter, Connective and MS Lesion. However, the number of classes varies along the z planes. The image is available in 181 different z planes. Fuzzy-VGAPS clustering algorithm is executed on the images projected on 7 different z-planes. The parameters of the algorithm are same as the above. The ground truth information is available to us. MS score [15]

is calculated after application of Fuzzy VGAPS-clustering technique in order to measure the ‘goodness’ of the solutions. Table II shows the actual number of clusters present in the image, the obtained number of clusters and the ‘goodness’ of the corresponding partitioning in terms of the MS Score after application of Fuzzy-VGAPS clustering algorithm on these 7 different MS Lesion Brain images. For the purpose of comparison, Fuzzy C-means algorithm [10] and EM algorithm [11] are again executed on these images, firstly with the number of clusters automatically determined by the Fuzzy-VGAPS and then with the actual number of clusters present in the images. The MS scores of the corresponding partitionings are also provided in Table II. The results again show that the MS-score corresponding to the partitioning provided by the Fuzzy-VAGPS clustering is, in general, the minimum. This again reveal the effectiveness of the Fuzzy-VGAPS clustering in automatically segmenting the MRI brain image with multiple sclerosis lesions. Figures 7(a),

8(a) and 9(a) show the original MS Lesion Brain image in T1 band projected on z2, z36 and z144 planes, respectively. Figures 7(b), 8(b), 9(b) show, respectively, the corresponding automatically segmented images obtained after application of Fuzzy-VGAPS clustering algorithm. The calculated MS scores show that the proposed Fuzzy VGAPS-clustering performs well in segmenting both normal brain image and brain image with multiple sclerosis lesions.

Further, experiments are carried out in order to establish the effectiveness of the symmetry based distance in Fuzzy-VGAPS clustering. Fuzzy-VGAPS without adaptive crossover and mutation operators (crossover probability=0.9, mutation probability=0.01) is now executed on the first 10 z planes of the MRI brain image with multiple sclerosis lesions. The corresponding MS scores are now provided in Table III. The results are then compared with those obtained by Fuzzy-VGA [12] (fuzzy variable string length genetic algorithm), optimizing popular Euclidean distance based Xie-Beni (XB) index [16], where Euclidean distance is used to compute the membership values of different points to different clusters. The number of clusters and the MS scores obtained by Fuzzy-VGA after applying it on the first 10 z planes of the MRI brain image with multiple sclerosis lesions are also provided in Table III. Results show that the proposed Fuzzy-VGAPS is more effective than the Fuzzy-VGA. This establishes the fact that the symmetry based distance is more effective in segmenting the MRI brain image than the existing Euclidean distance.

#### IV. DISCUSSION AND CONCLUSION

In this paper, the problem of automatic segmentation of MR images is posed as one of clustering in the intensity space. The search capability of the genetic algorithm is utilized for automatically evolving the cluster centers. The resultant partition matrix is associated with an optimum value of the fuzzy symmetry based validity index, *FSym*-index. Uncertainty in the medical image segmentation comes from imprecision in computations and vagueness in class definitions. Considering this, fuzzy set theory is incorporated for determining the membership values of different pixels to different clusters. In the proposed Fuzzy-VGAPS clustering technique, assignment of points to different clusters are made based on the newly proposed point symmetry distance rather than the Euclidean distance. This enables the proposed algorithm in identifying any types of clusters irrespective of its shape, size, convexity as long as the clusters possess the symmetry property. The proposed algorithm does not require the *a priori* specification of the number of clusters present in the data set. The effectiveness of the proposed algorithm is shown in segmenting several MRI brain images. The segmentation results are then compared with the available ground truth information. For the purpose of comparison, the well-known Fuzzy C-means and EM algorithms are also executed on these images. Experimental results show that Fuzzy-VGAPS clustering is not only able to automatically segment the MRI brain images into different tissue classes but the segmentation result is also the best than the two

well-known clustering algorithms quantitatively. The present Fuzzy-VGAPS clustering algorithm will not work well for the data sets having clusters whose centers collide at a same point.

As a part of the future work some spatial information will be incorporated while segmenting the brain MR images. Because due to the noise and intensity inhomogeneities introduced in imaging process, different tissues at different locations may have similar intensity appearance, while the same tissue at different locations may have a different intensity appearance. Therefore, sometimes the segmentation result will be improved after incorporating the spatial information. Authors are currently working in this direction.

#### REFERENCES

- [1] R. C. Gonzalez and R. E. Woods, *Digital Image Processing*. Massachusetts: Addison-Wesley, 1992.
- [2] P. Bradley, U. Fayyad, and C. Reina, "Scaling EM (expectation maximization) clustering to large databases," Microsoft Research Center, Tech. Rep., 1998.
- [3] Y. Zhang, M. Brady, and S. Smith, "Segmentation of brain MR image through a hidden markov random field model and the expectation maximization algorithm," *IEEE Transactions on Medical Imaging*, vol. 20, no. 1, 2001.
- [4] —, "A hidden markov random field model for segmentation of brain MR images," in *Proceedings of SPIE Medical Imaging 2000*, 2000, vol. 3979, pp. 1126–1137.
- [5] J. Suckling, T. Sigmundsson, K. Greenwood, and E. Bullmore, "A modified fuzzy clustering algorithm for operator independent brain tissue classification of dual echo MR images," *Magnetic Resonance Imaging*, vol. 17, pp. 1065–1076, 1999.
- [6] S. M. Bhandarkar and H. Zhang, "Image segmentation using evolutionary computation," *IEEE Transactions on Evol. Comp.*, vol. 3, no. 1, pp. 1–21, 1999.
- [7] M.-C. Su and C.-H. Chou, "A modified version of the k-means algorithm with a distance based on cluster symmetry," *IEEE Transactions Pattern Analysis and Machine Intelligence*, vol. 23, no. 6, pp. 674–680, 2001.
- [8] C. H. Chou, M. C. Su, and E. Lai, "Symmetry as a new measure for cluster validity," in *2nd WSEAS Int. Conf. on Scientific Computation and Soft Computing*, Crete, Greece, 2002, pp. 209–213.
- [9] S. Bandyopadhyay and S. Saha, "GAPS: A clustering method using a new point symmetry based distance measure," *Pattern Recog.*, Accepted (March, 2007), URL: <http://dx.doi.org/10.1016/j.patcog.2007.03.026>.
- [10] J. C. Bezdek, "Fuzzy mathematics in pattern classification," Ph.D. dissertation, Cornell University, Ithaca, NY, 1973.
- [11] A. K. Jain, M. Murthy, and P. Flynn, "Data Clustering: A Review," *ACM Computing Reviews*, Nov, 1999.
- [12] U. Maulik and S. Bandyopadhyay, "Fuzzy partitioning using a real-coded variable-length genetic algorithm for pixel classification," *IEEE Transactions Geoscience and Remote Sensing*, vol. 41, no. 5, pp. 1075–1081, 2003.
- [13] M. Srinivas and L. Patnaik, "Adaptive probabilities of crossover and mutation in genetic algorithms," *IEEE Transactions on Systems, Man and Cybernetics*, vol. 24, no. 4, pp. 656–667, April, 1994.
- [14] "BrainWeb: Simulated brain database." available: <http://www.bic.mni.mcgill.ca/brainweb>.
- [15] A. Ben-Hur and I. Guyon, *Detecting Stable Clusters using Principal Component Analysis in Methods in Molecular Biology*, M. Brownstein and A. Kohodursky, Eds. Humana press, 2003.
- [16] X. L. Xie and G. Beni, "A validity measure for fuzzy clustering," *IEEE Transactions on Pattern Analysis and Machine Intelligence*, vol. 13, pp. 841–847, 1991.